Structural Determinants for Activation or Inhibition of Ryanodine Receptors by Basic Residues in the Dihydropyridine Receptor II-III Loop

Marco G. Casarotto,*† Daniel Green,* Suzi M. Pace,* Suzanne M. Curtis,* and Angela F. Dulhunty*
*Division of Biochemistry and Molecular Biology, John Curtin School of Medical Research; and †Research School of Chemistry, Australian National University, Canberra, ACT 2601, Australia

ABSTRACT The structures of peptide A, and six other 7–20 amino acid peptides corresponding to sequences in the A region (Thr^{671}- Leu^{690}) of the skeletal muscle dihydropyridine receptor II-III loop have been examined, and are correlated with the ability of the peptides to activate or inhibit skeletal ryanodine receptor calcium release channels. The peptides adopted either random coil or nascent helix-like structures, which depended upon the polarity of the terminal residues as well as the presence and ionisation state of two glutamate residues. Enhanced activation of Ca^{2+} release from sarcoplasmic reticulum, and activation of current flow through single ryanodine receptor channels (at −40 mV), was seen with peptides containing the basic residues ^{681}Arg Lys Arg Arg Lys^{685}, and was strongest when the residues were a part of an α-helix. Inhibition of channels (at +40 mV) was also seen with peptides containing the five positively charged residues, but was not enhanced in helical peptides. These results confirm the hypothesis that activation of ryanodine receptor channels by the II-III loop peptides requires both the basic residues and their participation in helical structure, and show for the first time that inhibition requires the basic residues, but is not structure-dependent. These findings imply that activation and inhibition result from peptide binding to separate sites on the ryanodine receptor.

INTRODUCTION

Contraction in skeletal muscle depends on Ca^{2+} release from the sarcoplasmic reticulum (SR) through ryanodine receptor (RyR) calcium release channels. RyRs are activated during excitation-contraction coupling (ECC) by a signal originating in the plasmalemmal voltage sensor in the S4 segment of the α_1 subunit of L-type Ca^{2+} channels (dihydropyridine receptors, DHPRs). The signal initiates a protein/protein interaction with the RyR via the loop (II-III loop) between the second and third repeats of the skeletal DHPR (Tanabe et al., 1990). ECC in skeletal muscle is independent of external Ca^{2+}, and depends only on a correct interaction between the DHPR and RyR. Ca^{2+}-independent ECC cannot proceed if the DHPR is either absent, or of the cardiac type (Tanabe et al., 1990; Nakai et al., 1998). Interaction sites between the DHPR and RyR have been identified in the A region of the II-III loop between Glu^{671} and Leu^{690}, which binds to the RyR in surface plasmon resonance studies (O'Reilly and Ronjat, 1999) and in skeletal RyRs between Arg^{1076} and Asp^{1112}, which binds to the II-III loop (Leong and Maclennan, 1998). RyRs are activated by the skeletal DHPR II-III loop and by the 20 amino acid peptide A (Glu^{671}-Leu^{690}) (Lu et al., 1994, 1995; El-Hayek et al., 1995; Dulhunty et al., 1999a). Peptide A activates RyR channels at −40mV, but inhibits at +40mV; activation is thought to reflect peptide binding to a physiologically important DHPR binding site, whereas inhibition is consistent with peptide binding to negatively charged groups in the channel pore (Dulhunty et al., 1999a). Although inhibition is unlikely to occur in vivo because the II-III loop could not reach into the channel pore, the mechanism is important because it provides a potential tool for probing pore structure.

In intact muscle fibers, the peptide A region may facilitate binding of the II-III loop to the RyR, whereas other regions of the II-III loop transmit the ECC signal from the voltage sensor to the binding region (Dulhunty et al., 1999a). Thus activation of RyRs by peptide A, or by the II-III loop, may reflect binding to the RyR rather than activation equivalent to ECC (Dulhunty et al., 1999a). Indeed, activation of RyRs by the II-III loop occurs when the II-III loop has either the cardiac or the skeletal sequence (Nakai et al., 1998; Lu et al., 1994) and ECC in intact cells can proceed with a scrambled sequence in the A region (Proenza et al., 2000). It has been suggested that the highly charged ^{680}Arg Lys Arg Arg Lys^{685} region in peptide A is essential for RyR activation (El-Hayek and Ikemoto, 1998; Dulhunty et al., 1999b; Zhu et al., 1999).

The structure of the protein/protein interaction sites on the II-III loop and on the RyR is important for understanding the functional observations and structural changes that could occur during ECC. We have shown that peptide A is helical from its *N*-terminal end to Lys^{685}, but the C-terminal part is largely unstructured; the last turn of the helix, containing the essential basic residues, is poorly defined (Casarotto et al., 2000). A structural change after Ser^{687} Ala substitution extended the α-helix further to include the basic residues, and also enhanced the activation of RyRs by peptide A (Casarotto et al., 2000). We suggested that the greater ability of peptide A to activate RyRs after the

Received for publication 10 October 2000 and in final form 20 March 2001.

Address reprint requests to Dr. M. G. Casarotto, John Curtin School of Medical Research, Australian National University, PO Box 334, Canberra, ACT 2601, Australia. Tel: 61-2-6249-2598; Fax: 61-2-6249-0415; E-mail: marco.casarotto@anu.edu.au.

0006-3495/01/06/2715/12 $2.00

Ser^{687}Ala substitution was due to the increased helical content of the peptide. An alternative hypothesis that could not be excluded was that the enhanced activity of the Ser^{687}Ala-substituted peptide was due to the change in amino acid character rather than the structural change. Indeed, Ser^{687} has been shown by others to be important in activation of RyRs by the II-III loop (Lu et al., 1995). In the present study we sought to test the hypothesis that activation of RyRs at −40 mV by peptide A requires the ^{681}Arg Lys Arg Arg Lys^{685} residues and that activation is greater when the residues are structured in a helical form. The experiments also tested the hypotheses that inhibition of RyR activity at +40 mV by peptide A depends on the cluster of positively charged residues and that activation or inhibition of RyR channels depend on peptide A binding to different sites on the RyR. The structural and amino-acid sequence requirements of the potentially important inhibition process have not been previously examined, although it has been suggested that the positively charged residues might be involved in inhibition (Casarotto et al., 2000).

The ability of fragments of peptide A to activate (at −40 mV) or inhibit (+40 mV) RyR channels and to release Ca^{2+} from the SR was compared with the presence or absence of basic amino acids and with the helical content of the peptides (determined by nuclear magnetic resonance (NMR) and circular dichroism (CD)). Strongest activation was seen when the basic amino acids were present and had the greatest helical structure. In contrast, the ability of peptides to inhibit RyR channels depended only on the presence of the basic residues and was independent of helical structure.

EXPERIMENTAL PROCEDURES

Peptides

DHPR II-III loop peptides were synthesised as described in Dulhunty et al. (1999). Peptides used or referred to are:A1: ^{671}Thr Ser Ala Gln Lys Ala Lys Ala Glu Glu *Arg Lys Arg Arg Lys* Met Ser Arg Gly Leu^{690}; A2: ^{671}Thr Ser Ala Gln Lys Ala Lys Ala Glu Glu *Arg Lys Arg Arg Lys* Met *Ala* Arg Gly Leu^{690}; A3: ^{681}*Arg Lys Arg Arg Lys* Met Ser Arg Gly Leu^{690}; A4: ^{671}Thr Ser Ala Gln Lys Ala Lys Ala Glu Glu^{680}; A5: ^{675}Lys Ala Lys Ala Glu Glu *Arg Lys Arg Arg*^{684}; A6: ^{678}Ala Glu Glu *Arg Lys Arg Arg Lys* Met Ser^{687}; A7: ^{671}Thr Ser Ala Gln Lys Ala Lys Ala Glu Glu *Arg Lys Ala Val Ala* Met Ser Arg Gly Leu^{690}; and A9: ^{681}*Arg Lys Arg Arg Lys* Met Ser^{687}.

CD measurements

Precise concentrations of the peptide stocks were determined (Auspep Propriety, Ltd., Melbourne, Australia) using acid hydrolysis followed by a standardized phenylthiocarbamyl protocol. Samples were diluted to 25 μM for CD measurments, and the pH values adjusted to 3 and 6.5, with small additions of dilute HCl or NaOH. CD spectra were collected at 5°C on a Jobin Yvon CD6 Dichrograph (Cedex, France) using a cell path length of 1 mm. Ten spectra were collected per sample, averaged and then subjected to a smoothing function.

NMR spectroscopy

NMR samples were ~2 to ~3 mM in an H_2O solution containing 10% D_2O/90% H_2O. ^{1}H chemical shift values are given relative to 2,2-dimethyl-2-silapentane-5-sulfonate. The pH conditions for the NMR experiments were carefully adjusted with microliter additions of dilute (~0.5M) ^{2}HCl or NaO^{2}H. All spectra were acquired on Varian-Inova 600 and 500 spectrometers using spectral widths of 6000 and 5000 Hz, respectively, a pulse width of ~7 ms (90^o), and an acquisition time of 0.13 s, collecting 2048 data points and 512 increments of 32 transients. Nuclear Overhauser Effect Spectroscopy (NOESY) (Kumar et al., 1980) and Rotating Frame Overhauser Effect Spectroscopy (ROESY) (Bothner-By et al., 1984) spectra with a mixing time of 200 to 500 ms, Total Correlation Spectroscopy (TOCSY) (Bax and Davis, 1985) spectra with mixing times of 70 ms, and DQF-COSY (Rance et al., 1983) spectra were acquired at 5°C and used for the assignment of the ^{1}H-NMR resonances. Suppression of the H_2O resonance for the NOESY and DQF-COSY spectra was achieved using pulse field gradients (Piotto et al., 1992; Trimble et al., 1994), whereas water presaturation was employed for TOCSY and ROESY. The patterns of backbone hydrogen bonding were assessed by monitoring the chemical shift of the amide backbone protons with changes in temperature (4, 12, and 25°C) in TOCSY experiments (Deslauriers and Smith, 1980). The 2D data were processed on an O_2 Silicon graphics work station using the Felix 95 software package. Data sets were zero-filled to 4096 by 2048 K and multiplied by a phase-shifted sine-bell-squared function in both dimensions before transformation. $^3J_{NH\text{-}\alpha H}$ coupling constants were derived from 1D ^{1}H spectra where possible.

Ca^{2+} release from SR

Preparation of SR vesicles, Ca^{2+} release from SR and single channel techniques have been described (Dulhunty et al., 1999a). Rabbit skeletal SR vesicles (100 μg of protein) were added to a cuvette, to a final volume of 2 ml of a solution containing 100 mM KH_2PO_4 (pH = 7), 4mM $MgCl_2$, 1 mM Na_2ATP, and 0.5 mM antipyrylazo III. Extravesicular [Ca^{2+}] was monitored at 710 nm. Identical experiments at 790 nm showed no changes in Optical Density (OD) that would alter the rate of Ca^{2+} release measured at 710 nm.

Single channel techniques

Artificial lipid bilayers of PE, PS, and PC (5:3:2 w/w) (Avanti Polar Lipids, Alabaster, AL) were painted across a 100-μm diameter hole in a delrin cup, separating solutions containing *cis* (230 mM CsMS, 20 mM CsCl, 1 mM $CaCl_2$) or *trans* (30 mM CsMS, 20 mM CsCl, 1 mM $CaCl_2$); both with 10 mM [TES (pH 7.4) with CsOH] (Dulhunty et al., 1999a; Casarotto et al., 2000). For recording, (a) the *cis* solution was replaced with an identical solution, but with 10^{-4} M Ca^{2+}, and (b) 200 mM CsMS was added to the *trans* chamber. Channel activity was recorded, and mean current (I') measured, over a range of peptide concentrations at +40 mV and −40 mV. Potential was changed every 30 s and activity recorded for 2 min under each condition. Potential is expressed as $V_{cis} - V_{trans}$ (or $V_{cytoplasm} - V_{lumen}$). SR vesicles and peptides were added to the *cis* chamber at 20 to 25°C. Average data is given as mean ± SEM.

RESULTS

NMR studies of peptides

Complete ^{1}H assignments for peptides A4, A5, and A6 (at pH 3 and 5) and peptides A3 and A9 (at pH 3) are presented in Table 1 along with $^3J_{NH\text{-}\alpha H}$ coupling constants. These assignments were made using standard 2D methods, i.e., 2D TOCSY experiments to identify spin types and NOESY experiments to make sequence specific assignments. The amide region of the NOESY spectra for peptides A4, A5, and A6 are shown at pH 3 and 5 (Fig. 1). Backbone NH_i-NH_{i+1} NOE cross-peaks are visible for peptides A4, A5, and A6 at both pH values. At pH 3, peptide A4 shows weak NH_i-NH_{i+1} cross-peaks throughout the entire peptide chain, but shows a marked decrease in the number of NOEs at pH 5. The converse is true for peptide A6, where weak NH_i-NH_{i+1} NOEs are evident at pH 5, but absent at pH 3. The pH 3 and pH 5 spectra for peptide A5 shows only a few, relatively weak, cross-peaks, compared with either A4 or A6. No NH_i-NH_{i+1} cross-peaks occurred for A3 or A9 in either ROESY or NOESY spectra (not shown).

Secondary structural information can also be derived from the $^3J_{NH\text{-}\alpha H}$ coupling constants, α-proton chemical shift index (CSI) and hydrogen bonding information summarized in Fig. 2. Peptide A6 at pH 5 shows the greatest evidence of helical structure in that all NMR parameters strongly point to a helical conformation. For example, coupling constants for A6 were < 6 Hz, the temperature coefficients greater than −4.0 ppb (for the majority of the residues), and an upfield shift of the α protons are all compatible with a helix-type structure. Peptides A4 and A5 show some coupling-constant and temperature coefficient data, indicating potential helical character, but this is not seen in the CSI data. Peptides A3 and A9 do not show any of these characteristic helical traits, suggesting that both of these peptides adopt random coil structures in solution. These NMR results imply that, of the peptides studied, it is peptide A6 which exhibits the greatest helical content at pH 5; A4 and A5 show a small amount of helical structure and peptides A3 and A9 exhibit random coil structures.

Circular dichroism

CD spectra of peptides A1, A2, A4, A5, and A6 are shown at high (6.5) and low (3.0) pH to illustrate effects of protonation of glutamate residues, whereas traces for A3 and A9 (which lack glutamates) are shown only at high pH (Fig. 3). As expected from previous NMR results (Casarotto et al., 2000), A1 and A2 show profiles that are characteristically associated with helical-type structures. The greater minimum at 222 nm suggests that A2 is slightly more helical in structure than A1. The minimum at ~200 nm for A1 is significantly affected by a change in pH, whereas only a modest difference is seen in A2, indicating that ionisation of the glutamate residues plays a more significant role in stabilising the helix in A1 than in the A2 peptide. Both of these peptides also exhibit a positive band at ~185 nm, which is more prominent at higher pH values. A positive 185 nm region is also present for peptide A6, as is a minimum at ~200 nm. A clear spectral change at these wavelengths is observed with A6 when pH is lowered to 3.0, as is a slight reduction of the minimum at ~222 nm. All these changes indicate that the ionisation state of the glutamate residues act to stabilise the helix. Peptides A4, A5 A3 and A9 do not show a positive band at ~185 nm and have minimums that range from 195–197 nm. Only a modest shift in the minimum at 197 nm is observed for A5 with a change in pH, whereas the direction of the shift for A4 (~2 nm) is in the opposite direction to that seen with peptides A1, A2, and A6. No minimums are seen for peptides A4, A5 A3 and A9 at 222 nm, although a slight dip is seen for peptide A4 at low pH. This data indicates a helical order at high pH of A2>A1>A6>A4>A5>A3 = A9.

Ca^{2+} release from SR vesicles

SR vesicles were partially loaded with Ca^{2+} (Dulhunty et al., 1999a). Thapsigargin (200 nM) was then added to block Ca^{2+} uptake by the SR Ca^{2+}, Mg^{2+}-ATPase (first arrow in each inset Fig. 4) after which extravesicular Ca^{2+} increased slowly, due to Ca^{2+} leakage through RyRs. Peptide was added for ~3 min (second arrow). 5 μM *cis* ruthenium red (third arrow) then prevented further increases in extravesicular Ca^{2+}, showing that the increase in $[Ca^{2+}]$ was due to Ca^{2+} release through RyR channels. The Ca^{2+} ionophore A23187 (3 μg/ml), added at the fourth arrow, released the remaining Ca^{2+}, confirming that Ca^{2+} was available for release.

TABLE 1 Proton assignment for the A3, A4, A5, A6, and A9 peptide in 10%/90% D_2O/H_2O at 5°C

Residue	NH	Hα	Hβ	Other	$J_{(NH\text{-}\alpha H)}$ (Hz)
Peptide A3, pH 5					
Arg-681	8.50	4.31	1.82/1.75	Hγ 1.63/1.63, Hδ 3.21/3.21	
Lys-682	8.56	4.31	1.81/1.74	Hγ 1.46/1.40, Hδ 1.66/1.66, Hε 2.99	
Arg-683	8.45	4.23	1.80/1.75	Hγ 1.66/1.66, Hδ 3.21/3.21	6.4
Arg-684	8.55	4.30	1.76	Hγ 1.63/1.63, Hδ 3.21/3.21	
Lys-685	8.61	4.27	1.76/1.68	Hγ 1.46/1.40, Hδ 1.68/1.68, Hε 2.99	
Met-686	8.66	4.55	2.01/2.09	Hγ 2.55/2.62, Hε 2.00	
Ser-687	8.50	4.47	3.87/3.87		
Arg-688	8.63	4.37	1.89/1.80	Hγ 1.67/1.67, Hδ 3.22/3.22	
Gly-689	8.56	3.95			
Leu-690	8.37	4.30	1.67/1.67	Hγ 1.6, Hδ 0.88/0.93	7.4
Peptide A4, pH 3					
Thr-671	8.37	4.34	4.20	Hγ 1.23	
Ser-672	8.63	4.39	3.90/3.90		6.2
Ala-673	8.46	4.27	1.39		5.7
Gln-674	8.28	4.20	2.06/2.06	Hγ 2.39/2.39	6.6
Lys-675	8.37	4.21	1.83/1.76	Hγ 1.43/1.48, Hδ 1.66, Hδ 2.96/2.96	
Ala-676	8.31	4.23	1.39		
Lys-677	8.25	4.19	1.84/1.77	Hγ 1.45/1.45, Hδ 1.68, Hδ 3.00/3.00	6.4
Ala-678	8.31	4.23	1.39		
Glu-679	8.33	4.32	2.02/2.14	Hγ 2.52/2.52	
Glu-680	8.30	4.30	2.00/2.12	Hγ 2.48/2.48	
Peptide A4, pH 5					
Thr-671	8.36	4.35	4.23	Hγ 1.23	
Ser-672	8.59	4.42	3.89/3.89	6.2	
Ala-673	8.47	4.29	1.40		
Gln-674	8.33	4.23	2.07/2.00	Hγ 2.38/2.38	6.7
Lys-675	8.41	4.24	1.83/1.76	Hγ 1.47/1.47, Hδ 1.67, Hδ 3.00/3.00	
Ala-676	8.41	4.24	1.39		
Lys-677	8.36	4.25	1.83/1.77	Hγ 1.45/1.45, Hδ 1.68, Hδ 2.99/2.99	
Ala-678	8.46	4.27	1.39	6.5	
Glu-679	8.49	4.27	2.08/1.96	Hγ 2.34/2.34	
Glu-680	8.42	4.24	2.08/1.98	Hγ 2.33/2.33	
Peptide A5, pH 3					
Lys-675	8.42	4.20	1.81/1.76	Hγ 1.44/1.35, Hε 3.00	
Ala-676	8.50	4.27	1.38		
Lys-677	8.35	4.21	1.81/1.75	Hγ 1.43, Hδ 1.67, Hε 3.00	6.2
Ala-678	8.37	4.25	1.39		
Glu-679	8.44	4.28	2.07/1.99	Hγ 2.44/2.44	
Glu-680	8.41	4.27	2.00	Hγ 2.41/2.41	
Arg-681	8.47	4.27	1.84/1.77	Hγ 1.61, Hδ 3.19	7.8
Lys-682	8.37	4.25	1.82/1.76	Hγ 1.47, Hδ 1.69, Hε 3.00	6.0
Arg-683	8.42	4.27	1.79	Hγ 1.60, Hδ 3.19	
Arg-684	8.49	4.28	1.85/1.73	Hγ 1.69, Hδ 3.20	
Peptide A5, pH 5					
Lys-675	8.42	4.19	1.80/1.74	Hγ 1.47, Hδ 1.66, Hε 3.00	
Ala-676	8.52	4.27	1.40		
Lys-677	8.37	4.21	1.81/1.77	Hγ 1.49/1.45, Hδ 1.68, Hε 3.00	
Ala-678	8.41	4.23	1.41		
Glu-679	8.51	4.20	2.05	Hγ 2.41/2.34	
Glu-680	8.42	4.19	2.07	Hγ 2.41/2.34	
Arg-681	8.37	4.26	1.81/1.77	Hγ 1.68/1.62	
Lys-682	8.28	4.24	1.85/1.78	Hγ 1.49/1.39, Hδ 1.66, Hε 2.98	6.8
Arg-683	8.39	4.27	1.87/1.79	Hγ 1.70/1.63, Hδ 3.21	
Arg-684	8.39	4.27	1.87/1.79	Hγ 1.70/1.63, Hδ 3.21	

(continued)

TABLE 1 *(Continued)*

Residue	NH	Hα	Hβ	Other	$J_{(NH\text{-}\alpha H)}$ (Hz)
Peptide A6, pH 3					
Ala-678	8.51	4.15	1.39		4.7
Glu-679	8.64	4.26	2.01/2.08	Hγ 2.46/2.46	5.9
Glu-680	8.34	4.25	2.02/2.08	Hγ 2.46/2.46	5.9
Arg-681	8.28	4.22	1.83/1.83	Hγ 1.58/1.71, Hδ 3.18/3.23	6.5
Lys-682	8.24	4.24	1.78/1.85	Hγ 1.40/1.49, Hδ 1.67/1.67, Hε 2.99/2.99	6.4
Arg-683	8.31	4.27	1.78/1.86	Hγ 1.63/1.71, Hδ 3.20/3.20	6.3
Arg-684	8.40	4.27	1.79/1.84	Hγ 1.64/1.64, Hδ 3.20/3.20	6.6
Lys-685	8.48	4.27	1.78/1.85	Hγ 1.44/1.48, Hδ 1.70/1.70, Hε 3.00/3.00	6.5
Met-686	8.60	4.53	2.03/2.16	Hγ 2.56/2.65	6.9
Ser-687	8.36	4.42	3.89/3.89		7.1
Peptide A6, pH 5					
Ala-678	8.56	4.12	1.40		4.3
Glu-679	8.73	4.16	1.99/2.04	Hγ 2.31/2.31	5.7
Glu-680	8.40	4.15	2.00/2.04	Hγ 2.33/2.33	5.8
Arg-681	8.20	4.14	1.84/1.71	Hγ 1.60/1.60, Hδ 3.25/3.17	5.4
Lys-682	8.06	4.19	1.89/1.83	Hγ 1.51/1.40, Hδ 1.69/1.69, Hε 2.96/2.96	5.9
Arg-683	8.13	4.21	1.85/1.71	Hγ 1.62/1.62, Hδ 3.20/3.20	6.6
Arg-684	8.26	4.23	1.83/1.71	Hγ 1.64/1.64, Hδ 3.19/3.19	5.3
Lys-685	8.34	4.26	1.88/1.81	Hγ 1.48/1.38, Hδ 1.69/1.69, Hε 3.00/3.00	5.9
Met-686	8.49	4.50	2.04/2.04	Hγ 2.67/2.57, Hε 2.17	6.7
Ser-687	8.30	4.41	3.89/3.89		6.8
Peptide A9					
Arg-681	8.47	4.23	1.72/1.89	Hγ 1.36/1.54, Hδ 3.14	6.3
Lys-682	8.59	4.31	1.82	Hγ 1.44, Hδ 1.55, Hε 2.99	
Arg-683*	8.53	4.31	1.74/1.86	Hγ 1.42/1.59, Hδ 3.14	7.0
Arg-684*	8.57	4.29	1.78	Hγ 1.60/1.43, Hδ 3.14	
Lys-685	8.64	4.28	1.82/1.88	Hγ 1.37/1.47, Hδ 1.58, Hε 2.99	6.8
Met-686	8.74	4.57	2.01/2.16	Hγ 2.66/2.55	7.2
Ser-687	8.44	4.43	3.87/3.87		7.0

*Could not be definitively assigned due to ambiguity.
Several coupling constants are not listed due to peak overlap.

Average rates of peptide-enhanced Ca^{2+} release (the rate with peptide minus that with thapsigargin) are shown Fig. 4. The solid lines show average data for A1 (Dulhunty et al., 1999a), which we included for comparison. The insets show OD changes obtained with each peptide. A3, containing the basic ^{681}Arg Lys Arg Arg Lys^{685} sequence but lacking helical structure (above), caused a small increase in the rate of Ca^{2+} release at ~5 μM to ~15 μM (Fig. 4 *A*), but rates fell with higher concentrations. Peptide A4, lacking the five consecutive basic residues, but having some helical structural characteristics did not increase the rate of Ca^{2+} release (Fig. 4 *B*). Peptide A5, with four of the five basic residues, but little helical structure, evoked Ca^{2+} release (Fig. 4 *C*), but at a substantially lower rate than A6 (Fig. 4 *D*). A6 contained all five basic residues and had some structure. There was little increase in Ca^{2+} release with A7 (containing only two of the five basic residues); (Fig. 4 *E*) or with A9 (which, like A3, had all five basic residues but no helical structure) (Fig. 4 *F*). Data for A9 taken from Casarotto et al., 2000 (broken line in Fig. 4 *F*) is included for comparison. The order of peptides in releasing Ca^{2+} from SR was A6≥A1>A3>A5>A4 = A7 = A9.

Single RyR channel activity

The activity of single RyR channels, with 10^{-4} M *cis* Ca^{2+} with 2 mM *cis* MgATP, at −40 mV increases when peptide A (at concentrations between 100 nM and 50 μM) is added to the cis chamber, but is blocked at +40 mV (with peptide concentrations greater than 1 μM, (Dulhunty et al., 1999a). Single RyR channel activity in this study was also recorded at +40 mV and −40 mV, with 100 μM *cis* Ca^{2+} and 2 mM *cis* MgATP, to compare short peptide activity with peptide A activity. Potentials of +40 mV and −40 mV were used to separate the activating and inhibiting effects of the peptide and to compare each effect with peptide structure. A *cis* Ca^{2+} concentration of 100 μM was used because inhibition at +40 mV is most obvious with 100 μM *cis* Ca^{2+}, whereas activation is apparent over a range of *cis* Ca^{2+} from 100 nM to 10 μM (Dulhunty et al., 1999a).

The records in Fig. 5 show an increase in channel activity with A5 and A6 (−40 mV) and a decrease in channel activity with A3, A5, and A7 (+40 mV). Average normalized mean current (I′p/I′c, defined in the legend to Fig. 6) is also shown at −40 mV and +40 mV (Fig. 6). Published data for the native sequence (peptide A1) and peptide A9

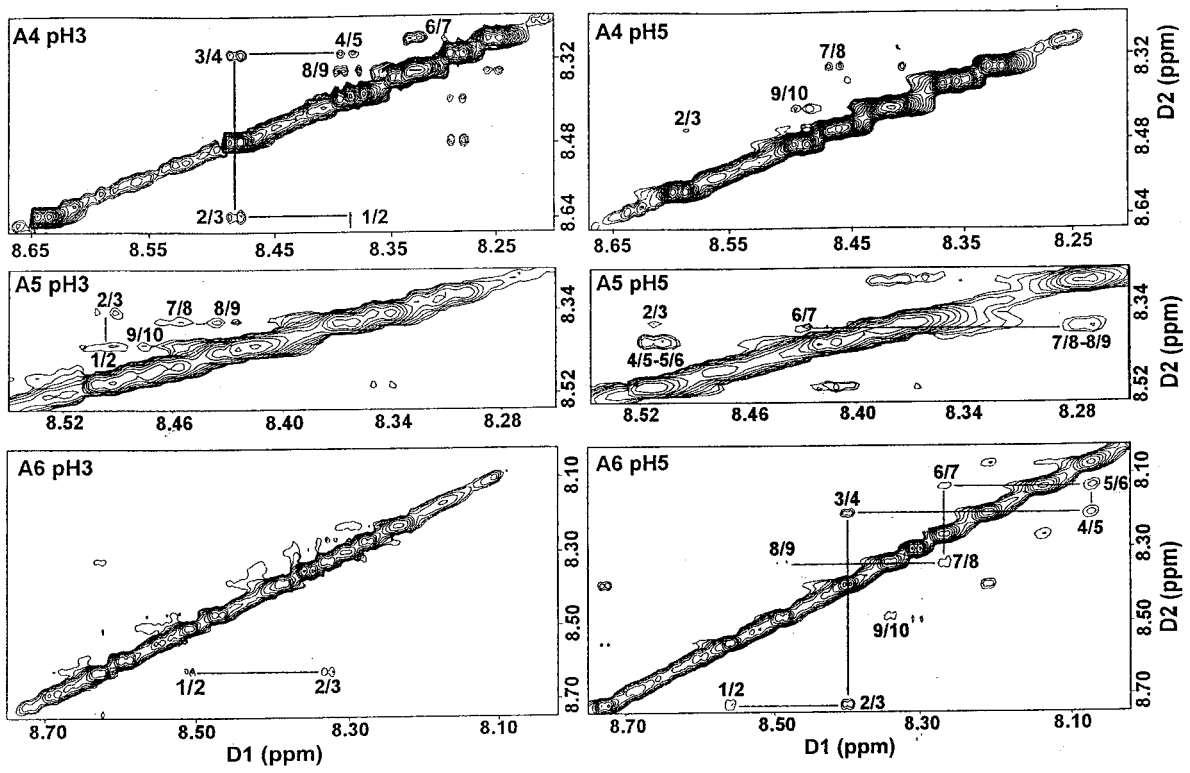

FIGURE 1 Amide-amide region of the NOESY spectra of peptides A4, A5, A6 at pH 3 and 5. Connected i-i+1 NOEs are shown and correspondingly labeled (residue 1 corresponds to the N-terminal residue) in the spectra.

(Dulhunty et al., 1999a) are included for comparison (small symbols, continuous lines in Fig. 6 *A–E*, and broken lines, Fig. 6 *E* respectively). The effects of the peptides on channel kinetics are shown in Fig. 7. Kinetic results are shown as nP_o, nT_o, nF_o, and nT_c so that data from many bilayers containing two channels (which often became apparent after peptide activation) could be included. It should be noted that bilayers containing only one channel showed the same relative changes in kinetics as bilayers containing two channels. Ruthenium red was added at the end of each experiment and abolished activity in all cases.

A3 and A5 caused small increases in channel activity at −40mV; both peptides contained the full basic sequence, but lacked helical structure. A greater twofold increase in I'p/I'c occurred with A6, which contained the five basic residues and was moderately structured. The increase in mean current was associated with significant increases in nP_o and nT_o (Fig. 7, −40mV). In contrast A4 which lacked the five sequential basic residues did not alter RyR activity. There was very little increase in mean current or nP_o with A7 (analysis data not included in Fig. 7) or A9. There was no change in single channel conductance with any of the peptides at −40mV. The order of the peptides in activating RyRs was A1>A6>A5>A3>A7 = A9 = A4.

Inhibition, a fall in channel activity at +40mV, was seen with A3, A5, A6, and A9, but not with A4 (Figs. 5–7). Inhibition by peptide A was characterized by reductions in the frequency, duration and amplitude of channel opening (Dulhunty et al., 1999a) and the same changes were seen with the short peptides (Fig. 7). Significant reductions in nP_o, nT_o and nF_o, and an increase in nT_c, were seen with A3, A6, and A9. No significant changes were seen with A7 (data not included). Curiously, an inhibiting decrease in nP_o and nT_o with A9 was seen at both +40mV and −40mV. The order of peptides in inhibiting RyRs was A3>A9>A1 = A6>A5>A7 = A4. Therefore, in contrast to activation, strongest inhibition was seen with peptides which contained ^{681}Arg Lys Arg Arg Lys^{685}, but not necessarily in a structured conformation.

DISCUSSION

This report examines the structure/function relationships of peptides corresponding to the peptide A region of the II-III loop of the skeletal DHPR α_1 subunit. We previously found that increasing the helical content of the C-terminal end of peptide A, by a Ser^{687} to Ala substitution increased the ability of the peptide to activate skeletal RyRs and we suggested that the greater helical structure may be responsible for enhanced RyR activation (Dulhunty et al., 1999a;

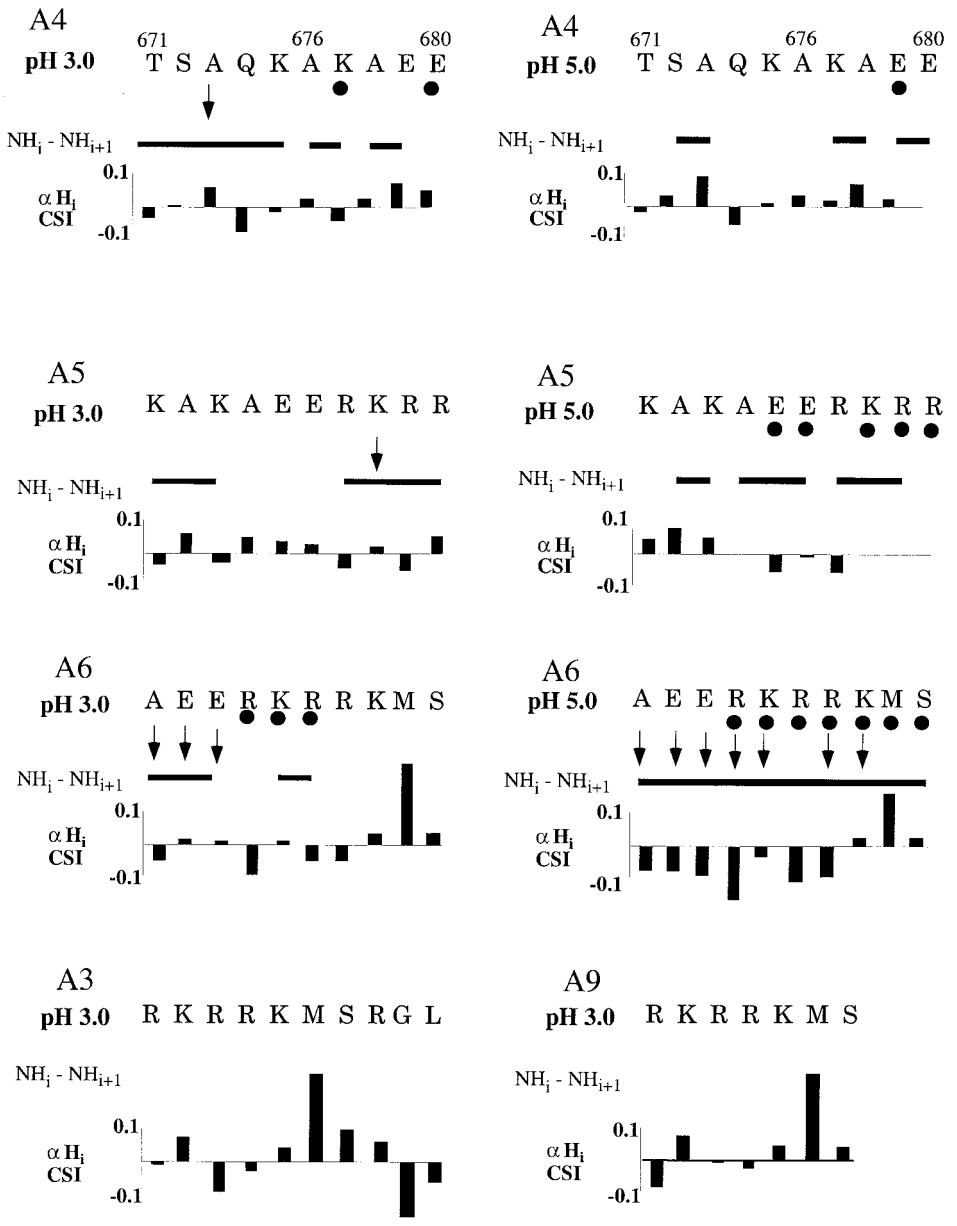

FIGURE 2 Summary of the sequential NH_i-NH_{i+1} NOE connectivities, $^3J_{NH\text{-}\alpha H}$ coupling constants, α-proton chemical shift index (CSI[1]) and temperature coefficients at 5°C in 10%/90% D_2O/H_2O for peptides A3, A9 (pH 3) and A4, A5, A6, and A9 (pH 3 and 5). The NOE connectivities are indicated by horizontal black lines with thickness proportional to NOE intensity. Values of $^3J_{NH\text{-}\alpha H} \leq 6$ Hz are indicated by $\downarrow$. Temperature coefficients > -4.0 ppb are represented by closed circles. The CSI shows the αH chemical shift of residues which deviate from random coil values (Wishart et al., 1991).

Casarotto et al., 2000). This hypothesis has been explored in the present study, in which we constructed different peptides fragments in order to examine the influence of the five basic residues (^{681}Arg Lys Arg Arg Lys^{685}) on activity and helical structure.

Structural observations

Although short peptides are most likely to adopt a random coil structure, both NMR and CD spectra suggested that some of the short peptides examined here tend to adopt a nascent helix-type conformation (i.e., an interconverting mixture of random coil and structured peptide). This assertion is based on the presence of NOEs between amide to amide protons (NH_i-NH_{i+1}), indicating an α-helix, but the absence of weaker NOEs synonymous with helical structure (i.e., NH_i-NH_{i+2},αH_i -NH_{i+3}, or αH_i -βH_{i+3}). Other NMR parameters such as $^3J_{NH\text{-}\alpha H}$ coupling constants, α-proton chemical shift index (CSI[1]), and hydrogen bonding data also support a helical-like structure. The CD profile for an ideal

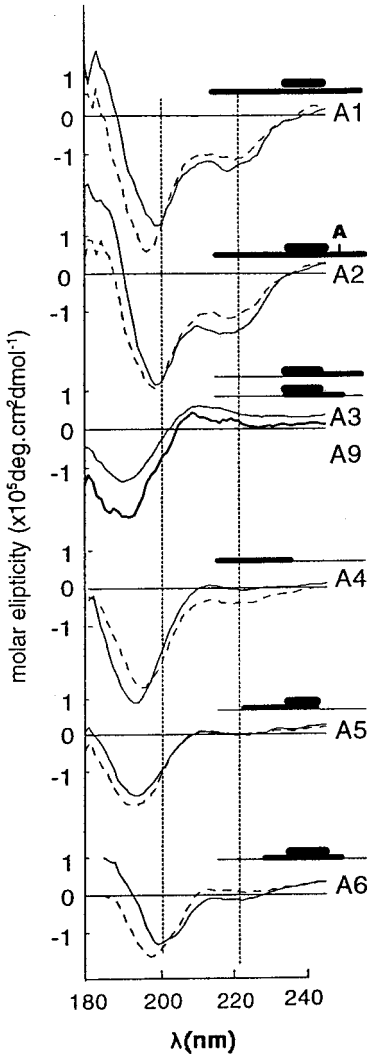

FIGURE 3 CD spectra at 5°C of solutions of peptide A3, A4, A5, A6, and A9 (concentrations of 2.5×10^{-5} M). Solid lines denote spectra acquired at pH 6.5 and broken lines at pH 3.0. Both spectra for A3 and A9 were acquired at pH 6.5. The thin line is for A3 and the thick line for A9. Vertical dotted lines are drawn at 200-nm and 222-nm. The peptide structure is indicated by the bars above each set of records. The thin bar shows the full length peptide A, medium bar shows the position and length of each particular peptide and the short bar indicates the position and number of positively charged residues from the ^{681}Arg Lys Arg Arg Lys^{685} sequence.

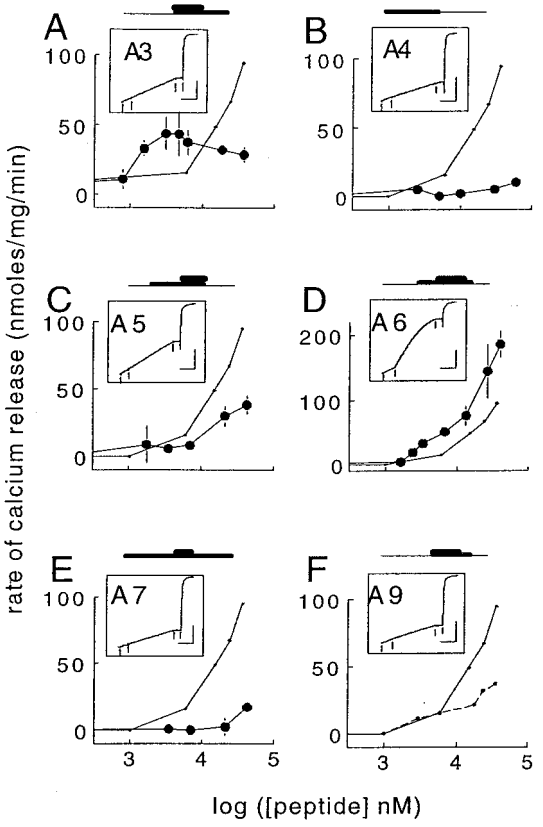

FIGURE 4 Effect of peptides on Ca^{2+} release from SR. (*A-F*) show initial rates of Ca^{2+} release (nmol/mg of TC vesicles/min) induced by peptides, i.e., the initial rate with peptide, minus the preceding rate with thapsigargin. The large circles are means ± SEM ($n = 3$, three different SR preparations). Small filled circles (*continuous lines*) show average data for the native A1 (Dulhunty et al., 1999a) and the small open circles in (*F*) (*dashed lines*) show average data for peptide A9 (Casarotto et al., 2000), both included for comparison. The insets are records of OD changes at 710 nm. The first arrow indicates addition of 200nM thapsigargin and the second addition of (in μM): (*A*) 5, A3; (*B*) 30, A4; (*C*) 60, A5; (*D*) 60 A6; (*D*) 60 A7 and (*F*) 60 A9. Ruthenium red (10 μM) was added at third arrow, before the ionophore A23187 (last *arrow*, 3 μg/ml). The vertical calibration is 0.1 OD unit [addition of 10 μM Ca^{2+} (or 20 nmoles) increased OD by 0.1 unit]. The horizontal calibration is 1 min. The peptide segment of A is indicated by the bars above each set of records (described in the legend to Fig. 3).

helix exhibits a positive band at 190 nm, and minimums at 208 and 222 nm (Woody and Tinco, 1967). Some peptides showed minimums near 200 and 222 nm, as well as a positive band near 185 nm. Such profiles represent deviations from the ideal profile, supporting the concept of a mixture of helix and random coil structure. The NMR and CD indicators, when combined, form a compelling argument for the presence structures which contain helix-like characteristics for some of the peptides. Because of the lack of well defined helices, the solution structures of the peptides were not accurately determined. However, a qualitative assessment of the level of helical content can be made.

High resolution solution structures of peptides A1 and A2 from NMR (Casarotto et al., 2000) show a greater helical content for A2 than A1, which is confirmed here by the more pronounced CD minimum at 222 nm, and a greater positive region at 185 nm observed in A2 compared to A1. The effects of pH on the spectra for the two peptides reveals that the glutamate residues aid in stabilization of the helix at high pH, via side chain interactions between the glutamate and arginine/lysine residues. The irregular helical structure of A1 is more susceptible than the more regular helical conformation of A2 to removal of the side chain-side chain

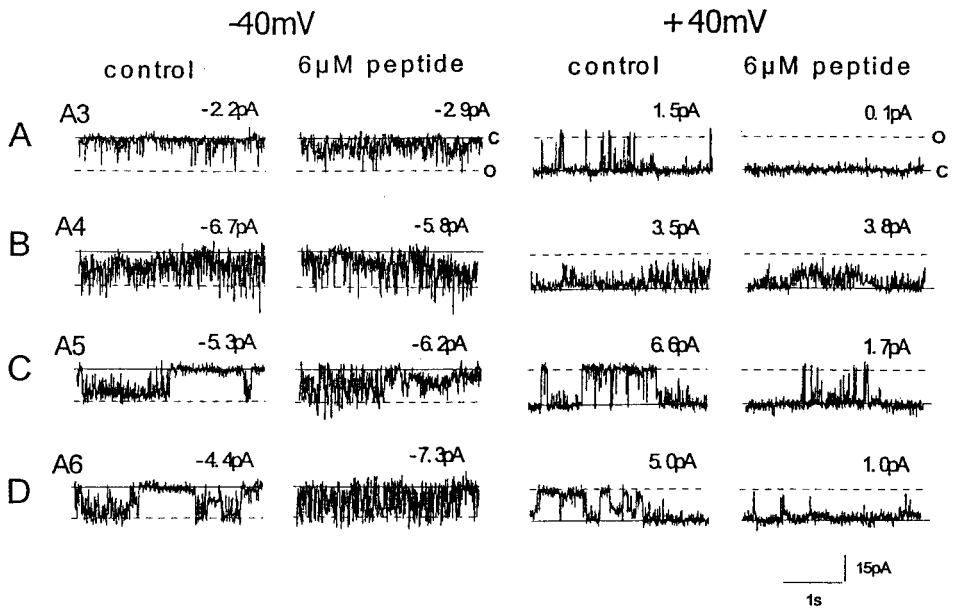

FIGURE 5 Single channel activity at −40mV and +40mV, before (control) and after (6 μM peptide) addition of 6 μM peptide to the *cis* solution bathing bilayers containing RyR channels. The mean current from a 30 s recording is shown at the top right hand corner of each record. Peptides added were A3 (*A*), A4 (*B*), A5 (*C*) and A6 (*D*). The continuous line in each record shows the closed channel current (labeled C). The broken line shows the maximum open channel conductance (labeled O).

interactions at pH 3. This suggests that A1 relies much more than A2 on the side chain-side chain interactions to maintain its helical integrity.

Apart from A1 and A2, one other peptide with substantial helical content was A6 at pH above the pK_a value of the glutamate residues. The helical nature of A6 at high pH is indicated by a complete set of NH_i-NH_{i+1} NOEs, $^3J_{NH\text{-}\alpha H}$ coupling constants, α-proton chemical shift index (CSI), and hydrogen bonding, whereas a positive band at ~185 nm, minimum at ~200 nm, and a slight minimum at ~222 nm are apparent in the CD spectrum. The loss of the helix-indicating NMR parameters at low pH, the disappearance of the positive 185 nm band, and the shift in CD minimums at 199 nm to lower wavelengths (~197 nm) show that protonation of the glutamates does play a helix stabilizing role. A similar feature was observed for peptides A1 and A2, in which the negatively charged glutamate and lysine/arginine residues (681–685) were found to stabilize the helix (Casarotto et al., 2000).

Compared to peptide A6, the opposite effect was seen for A4, in which evidence of a modest amount of helical character was observed for A4 at low pH but not at high pH. Indeed, the presence of NH_i-NH_{i+1} NOEs in the NOESY experiment at low pH suggests that all A4 residues participate in the formation of a respectable α-helix. This fact is supported not only by NOE evidence, but by CD minimum at 198 nm and the shallow, broad minimum at 222 nm at pH 3. The helical component was diminished at high pH, indicated by loss of NMR helical indicators and a shift in the CD spectrum minimum from 198 to197 nm. This may be due to destabilization of the helix by unfavorable interactions between the negative side chains of the ionized terminal glutamate residues (pH >4), and the natural negative dipole of the C-terminal end of the helix (Vieille and Zeikus, 1999). This interaction is removed upon protonation of the glutamate side chains at pH 3.

Peptide A5 shows little if any structure at high or low pH, and A3 and A9 were unstructured. The lack of structure of A5 was surprising since it contained both glutamate and arginine/lysine residues, but may be explained by destabilizing interactions between the natural dipole of the helix and the basic residues at the N-terminus of the peptide disrupting the Glu/Lys-Arg interactions. Similar destabilizing interactions would occur in the unstructured A3 and A9 peptides that, in conjunction with the absence of glutamate residues, would lower the probability of helix formation.

These findings show that of the short peptides, it is A6 at high pH which displays the greatest structural characteristics which are consistent with an α-helix. This, in part, is due to the amino acid composition; particularly the stabilizing effect of the charged residues at either end of the helix and the ionic involvement of the acidic glutamate residues with the basic residues in the sequence. The tendency of these shorter peptides to form α-helices at high pH can be summarized as follows: A6>A4>A5>A3 = A9.

Activation of Ca^{2+} release and RyR channels at −40mV

Our results confirm previous studies which suggested that the five basic residues (^{681}Arg Lys Arg Arg Lys^{685}) are necessary for RyR activation by peptide A (El-Hayek and Ikemoto, 1998; Dulhunty et al., 1999b; Zhu et al.,

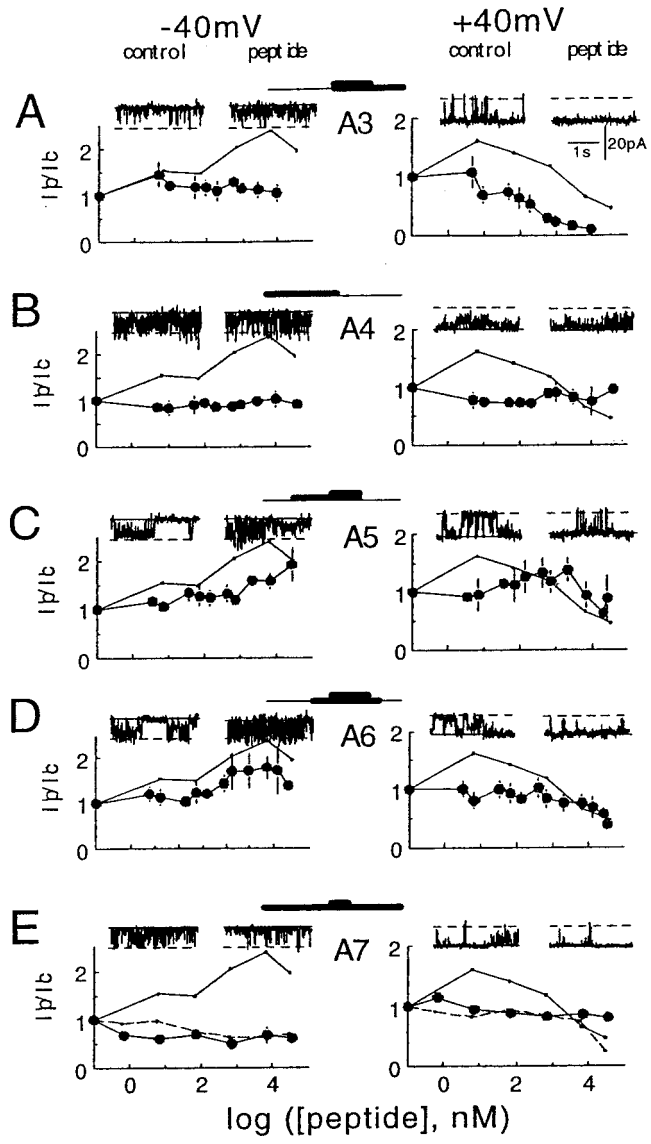

FIGURE 6 Effects of peptides on relative mean current flowing through RyRs at −40 mV and +40 mV. (*A–E*), relative mean current (I′p/I′c, see text) is plotted against the logarithm of [peptide A] in nM. Symbols show average I′p/I′c and vertical bars show ±1 SEM where this is greater than the dimensions of the symbol. 100 μM Ca^{2+} and 2mM MgATP were present in *cis* solution: (*A*) −A3 (n = 6); (*B*) −A4, (n = 5); (*C*) −A5 (n = 8); (*D*) −A6, (n = 15); (*E*), A7, (n = 8). The small filled circles (*continuous lines*) show average data for A1 (Dulhunty et al., 1999a) and small open circles in (*E*) (*dashed lines*) show average data for A9 (Casarotto et al., 2000), both included for comparison. The records above each graph give data shown in Fig. 6 and are included for comparison. The peptide segment of A is indicated by the bars above each set of records (described in the legend to Fig. 3).

1999). Peptide A4, which lacks the residues, was inactive, whereas A3, which contains the residues, showed activity. However, in contrast to El Hayek and Ikemoto (El-Hayek and Ikemoto, 1998), we found that the C-terminal half of peptide A (A3) (equivalent to AS10) is both a poor activator of RyR channels and is not very effective in releasing Ca^{2+} from SR vesicles. The differences may lie in the different techniques used. The previous studies examined tritiated ryanodine binding rather than single RyR channel activity and used a faster spectrophotometric technique than that used in our studies.

The low activity of A3 here, in conjunction with the unstructured nature of the peptide, is consistent with trends seen with the other peptides, and is also consistent with the hypothesis that the ability of peptides to bind to the RyR and increase its activity depends on a helical structure. The increase in Ca^{2+} release from the SR, and in channel activity at −40 mV with low [A3] could be because shorter unstructured peptide can more easily approach the binding pocket of RyRs in SR vesicles, but once there, binds less effectively.

Block of channel activity

A fall in RyR activity at +40 mV is seen with peptide A at >1 μM, and is thought to be due to peptide action at a second site on the RyR because its characteristics differ from those of activation at −40 mV. Reduced channel conductance during the inhibition, its voltage-dependence and its sensitivity to the direction of current flow are consistent with the peptide entering and blocking the channel pore, as positively charged groups on the peptide bind to negatively charged groups in the vestibule (Dulhunty et al., 1999a).

We show here that inhibition indeed depends on the positive charge density in the peptide. No inhibition was seen with A4, although it contains two lysine residues, or with A7, which contained two of the five sequential basic residues. Some inhibition was seen with A5, having four of the five residues, and stronger inhibition seen with A1 and A6 (containing the five residues in a structured conformation). Strongest inhibition was seen with the unstructured A3 and A9, perhaps because the five positively charged residues were free to form multiple random associations with scattered negative charge near the pore (Mead et al., 1998). The fact that inhibition was greatest when the basic residues were unstructured provides further evidence that activation and inhibition result from peptide binding to different sites. Activation is likely to depend on specific binding of the peptide to a pocket in the RyR that is designed to accept positively charged residues in a helical structure.

In summary, we show here that, by controlling the composition of peptides derived from the DHPR II-III loop to include residues (^{681}Arg Lys Arg Arg Lys^{685}), we are able to influence the level of helical structure imparted on the peptide. This is best illustrated in peptides A1, A2 and A6 where helical content is controlled by the amino acid composition of these peptides. Key amino acid features for these three peptides were found to include strategically important glutamate and arginine/lysine residues as well as helix dipole stabilizing resi-

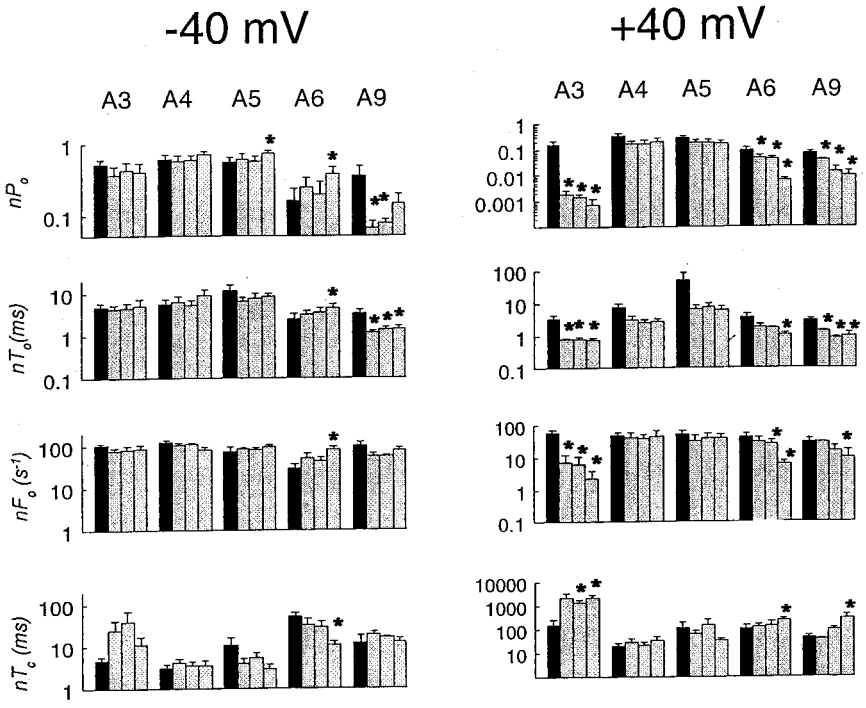

FIGURE 7 Single channel parameters recorded under control conditions and in the presence of each of peptides A3, A4, A5, A6 and A9 as indicated, at −40 mV (left side) and +40 mV (right side). The graphs show average data for nP_o, nT_o, nF_o, and nT_c plotted on a logarithmic scale to show changes in channel activity over the wide range of values recorded during activation and inhibition. Data was recorded for 2 min under control conditions at each peptide concentration, between 15 and 135 s after peptide addition. Sixty seconds of data was obtained at −40 mV and 60 s at +40 mV. The full 60 s of data was analyzed. The black bins show control data, and the grey bins data obtained with increasing peptide concentrations (0.6, 1.8, and 6 μM). The numbers of bilayers were the same as those for Fig. 6. Asterisks show data that is significantly different from control (Students *t*-test, $p < 0.05$).

dues at the terminal ends. The helical structure of the basic residues (^{681}Arg Lys Arg Arg Lys^{685}), in turn, controls the amount of activation of Ca^{2+} release from the SR and amount of RyR regulation. In addition we found that inhibition by peptide A at −40 mV depends on the presence of these five basic residues, and that it is greatest when peptides (A3 and A9) have the least structure.

REFERENCES

Bax, A., and D. G. Davis. 1985. MLEV-17 based two dimensional homonuclear magnetisation transfer spectroscopy *J. Magn. Reson.* 65: 355–360.

Bothner-By, A. A., R. L. Stephens, J. Lee, C. O. Warren, and R. W. Jeanloz. 1984. Structure determination of a tetrasaccharide-transient nuclear Overhauser effects in the rotating frame. *J. Am. Chem. Soc.* 106:811–3.

Casarotto, M. G., F. Gibson, S. M. Pace, S. M. Curtis, M. Mulcair, and A. F. Dulhunty. 2000. A structural requirement for activation of skeletal RyRs by a 20 amino acid region of the II-III loop of the skeletal DHPR. *J. Biol. Chem.* 275:11631–11637.

Dulhunty, A. F., D. R. Laver, E. M. Gallant, M. G. Casarotto, S. M. Pace, and S. Curtis. 1999a. Activation and inhibition of skeletal RyR channels by a part of the skeletal DHPR II-III loop: effects of DHPR Ser687 and FKBP12. *Biophys. J.* 77:189–203.

Dulhunty, A. F., S. M. Pace, and S. M. Curtis. 1999b. Residues in the skeletal DHPR II-III loop that activate or inhibit skeletal RyRs. *Biophys. J.* 76:a466.

El-Hayek, R., B. Antoniu, J. Wang, S. L. Hamilton, and N. Ikemoto. 1995. Identification of calcium release-triggering and blocking regions of the II-III loop of the skeletal muscle dihydropyridine receptor. *J. Biol. Chem.* 270:22116–22118.

El-Hayek, R., and N. Ikemoto. 1998. Identification of the minimum essential region in the II-III loop of the dihydropyridine receptor a1 subunit required for activation of skeletal muscle-type excitation-contraction coupling. *Biochemistry.* 37:7015–7020.

Kumar, A., R. R. Ernst, and K. Wuthrich. 1980. A two–dimensional nuclear overhauser enhancement (2D nOe) experiment for the elucidation of complete proton-proton cross-relaxation networks in biological molecules *Biochem. Biophys. Res. Commun.* 95:1–6.

Leong, P., and D. H. Maclennan. 1998. A 37-amino acid sequence in the skeletal muscle ryanodine receptor interacts with the cytoplasmic loop between domains II and III in the skeletal muscle dihydropyridine receptor. *J. Biol. Chem.* 273:7791–7794.

Lu, X., L. Xu, and G. Meissner. 1994. Activation of the skeletal muscle calcium release channel by a cytoplasmic loop of the dihydropyridine receptor. *J. Biol. Chem.* 269:6511–6516.

Lu, X., L. Xu, and G. Meissner. 1995. Phosphorylation of dihydropyridine receptor II-III loop peptide regulates skeletal muscle calcium release channel function. *J. Biol. Chem.* 270:18459–18464.

Mead, F. C., D. Sullivan, and A. J. Williams. 1998. Evidence for a negative charge in the conduction pathway of the cardiac ryanodine receptor channel provided by the interaction of K^+ channel N-type inactivation peptides. *J. Membr. Biol.* 163:225–234.

Nakai, J., T. Tanabe, T. Konno, B. Adams, and K. G. Beam. 1998. Localization in the II-III loop of the dihydropyridine receptor of a sequence critical for excitation-contraction coupling. *J. Biol. Chem.* 273:24983–24986.

O'Reilly, F. M., and M. Ronjat. 1999. Direct interaction of the skeletal dihydropyridine receptor α1 subunit with skeletal and cardiac ryanodine receptors. *Biophys. J.* 76:*A*466(Abstr).

Piotto, M., V. Saudek, and V. Sklenar. 1992. Gradient tailored excitation for single-quantum nmr spectroscopy of acqueous solutions. *J. Biomol. NMR.* 2:661.

Proenza, C., C. M. Wilkins, and K. G. Beam. 2000. Excitation-contraction coupling is not affected by scrambled sequence in residues 681–690 of the dihydropyridine receptor II-III loop. *J. Biol. Chem.* 275:29935–7.

Rance, M., O. W. Sorensen, G. Bodenhausen, G. Wagner, R. R. Ernst, and K. Wuthrich. 1983. Improved spectral resolution in cosy ^{1}H NMR

spectra of proteins via double quantum filtering. *Biochem. Biophys. Res. Commun.* 117:479–83.

Tanabe, T., K. G. Beam, B. A. Adams, T. Niidome, and S. Numa. 1990. Regions of the skeletal muscle dihydropyridine receptor critical for excitation-contraction coupling. *Nature.* 346:567–568.

Trimble, L. A., and M. Bernstein. 1994. Applications of gradients for water supression in 2D multiple quantum filtered cosy spectra of peptides. *J. Magn. Reson.* 105:67–72.

Vieille, C., and J. G. Zeikus. 1996. Thermoenzymes- identifying molecular determinants of protein structural and functional stability. *Trends Biotechnol.* 14:183–90.

Wishart, D. S., B. D. Sykes, and F. M. Richards. 1991. Relationship between nuclear magnetic resonance chemical shift and protein secondary structure. *J. Mol. Biol.* 222:311–33.

Woody, R. W., and I. Tinco, Jr. 1967. Optical rotation of orientated helices. III. Calculation of the rotatory dispersion and circular dichroism of the alpha- and 3_{10}-helix. *J. Chem. Phys.* 46:4927–45.

Zhu, X., G. Gurrola, M. T. Jiang, J. W. Walker, and H. H. Valdivia. 1999. Conversion of an inactive cardiac dihydropyridine receptor II-III loop segment into forms that activate skeletal ryanodine receptors. *FEBS Lett.* 450:221–226.